International Journal of Medical, Medicine and Health Sciences
ISSN: 2517-9969
Vol:4, No:4, 2010

Electromagnetic Field Modeling in Human Tissue

Iliana Marinova, Valentin Mateev

***Abstract*—**For investigations of electromagnetic field distributions in biological structures by Finite Element Method (FEM), a method for automatic 3D model building of human anatomical objects is developed. Models are made by meshed structures and specific electromagnetic material properties for each tissue type. Mesh is built according to specific FEM criteria for achieving good solution accuracy. Several FEM models of anatomical objects are built. Formulation using magnetic vector potential and scalar electric potential (A-V, A) is used for modeling of electromagnetic fields in human tissue objects. The developed models are suitable for investigations of electromagnetic field distributions in human tissues exposed in external fields during magnetic stimulation, defibrillation, impedance tomography etc.

***Keywords*—**electromagnetic field, finite element method, human tissue.

I. Introduction

COMPUTER modeling of electromagnetic fields distributed in biological objects is of paramount importance for investigations of processes and phenomena during medical diagnosis and therapy. Finite element method (FEM) is a powerful numerical method capable to solve such complex problems as electromagnetic field distributions in biological structures taking into account all characteristics and special features. Recent achievements of the FEM give possibilities to model fully three-dimensional, nonlinear, nonhomogenius, or anisotropy multi-tissue, and multi-joint systems of biological objects.

In order to achieve accurate field distribution results the realistic 3D geometry models are needed. The data from several imaging systems, such as CT, MRI, Ultrasound, are used for building of exact anatomical model. Recently, different techniques have been developed to convert automatically 3D image data into 3D FEM models or into numerical meshes suitable for FEM analysis [1-4, 6-17].

In this paper a method for automatic 3D model building of the various parts and organs of the human body suitable for FEM modeling is developed. The geometry models are made by image slices data acquired by CT. Finally the geometry models present the human anatomy as mesh structures. Mesh is built according to specific FEM criteria for achieving good solution accuracy. Also, electromagnetic properties of live tissue are needed for determination of exact field distributions. The specific electromagnetic material properties are introduced for each tissue of the developed model. Concept of computerized measurement system for electromagnetic field property determination is proposed.

FEM formulation using magnetic vector potential and scalar electric potential (A-V,A) is applied for modeling of electromagnetic field distributions in built models of human organs. The analysis is made by ANSYS software [5].

The developed 3D model building method is implemented for field distribution investigation during magnetic stimulation.

I. Marinova is with the Department of Electrical Apparatus, Faculty of Electrical Engineering, Technical University of Sofia, Bulgaria (phone: +359 2 965-3873; e-mail: iliana@ tu-sofia.bg).

V. Mateev is with the Department of Electrical Apparatus, Faculty of Electrical Engineering, Technical University of Sofia, Bulgaria (e-mail: vmateev@tu-sofia.bg).

II. 3D Model Building

Method for 3D model building of the human parts and organs is developed. The structure of the method is shown in Fig.1. As input a sequence of 2D slices acquired by visual diagnostic equipment (ultrasound, CT or MRI) are used. Application of image processing techniques essentially enhances the image properties.

The basic steps of 3D model building method are data acquisition, segmentation, element decomposition, volume generation and property association.

Acquired 2D slices are collected in a 3D image stack. This stack is used for generation of 3D voxel Data Base (DB). All image and data processing are done over that 3D voxel DB.

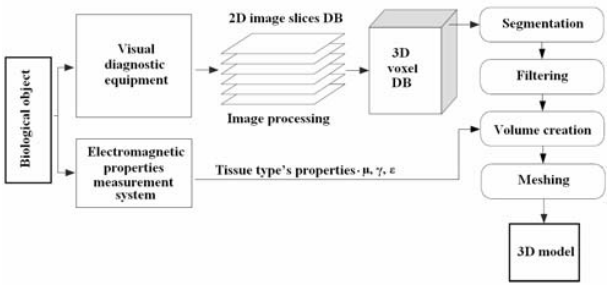

Fig. 1 Structure of the method for model building

Segmentation of 3D image DB is the process of tissues and their boundaries identification. This process is quite time consuming especially when large data sets are used. In such

cases automation of segmentation procedures is required. Here, organs segmentation is made semiautomatic by recognizing their contours in the 3D voxel DB. Tissue segmentation is made by voxel intensity histogram shown in Fig.2. Each tissue type is associated by its intensity level depending of used diagnostic equipment.

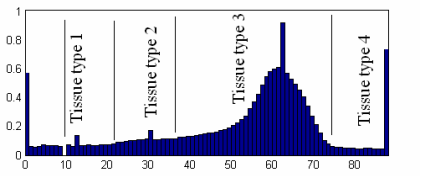

Fig. 2 Voxel intensity histogram for tissue segmentation

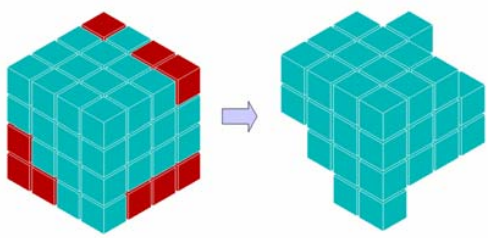

Fig. 3 Slices stack filtration.

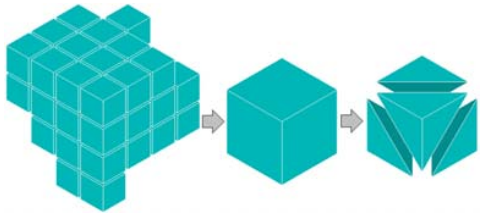

Fig. 4 Voxels decomposition process

Segmentation filtering procedure is applied for tissue separation. Intensity histogram, shown in Fig. 2, is used for separation where uncommon voxels are excluded from organ database. As output of that stage voxel databases are separated for each tissue type.

After that each voxel is decomposed in five tetrahedrons as shown in Fig.4. These tetrahedrons form the initial mesh representing the solid anatomy geometry.

For volume creation the tetrahedrons are assembled together. External tetrahedrons could be deleted for smooth model surface. In that stage the solid volumes representing the different tissue types are separated. Solid volumes are collected together in common coordinate system and elements numbering.

The generated geometry model is imported in FEM software where it is treated as volume object. Imported volumes are associated with corresponding electromagnetic material properties.

For method demonstration a 3D model of a part of a cardiac muscle is build. The sequence of 2D slices is acquired by ultrasound scanner.

In image segmentation the heart muscle position and external boundaries are pointed. Heart tissue is filtered by its image intensity. Stack with 22 slices is used. The distance between slices is 5 mm. Part of the slice stack is shown in Fig.5. Three dimentional slice stack is shown in Fig.6. In Fig. 7 and Fig. 8 are given the reconstructed volume and meshed volume of human heart, respectively.

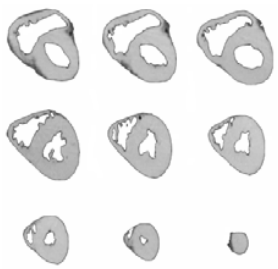

Fig. 5 2D slice sequence of human heart

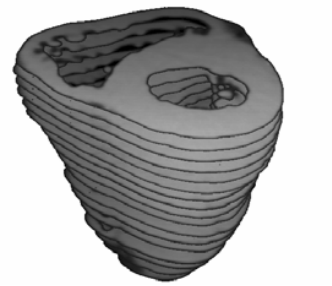

Fig. 6 3D slices stack assembly of human heart

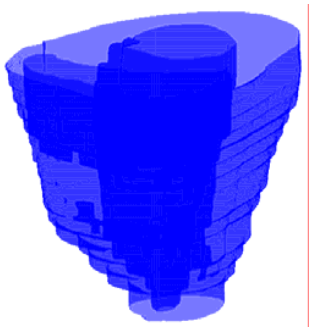

Fig. 7 Reconstructed volume of human heart

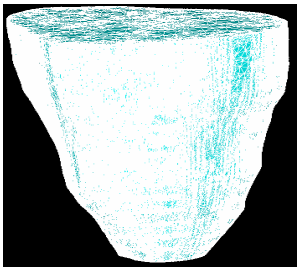

Fig. 8 . Meshed volume of human heart

III. Electromagnetic Properties

For modeling of electromagnetic fields the electromagnetic properties of biological tissue as electric permittivity - ε, magnetic permeability -μ and electric conductivity – σ, have to be imbedded into 3D models of human parts and organs. This is made for every solid volume which represents the unique tissue type for each organ modeled. In fact electric conductivity and permittivity are functions of frequency and have a very width range of variations according to reference sources. For accurate properties determination a computerized measurement system is developed.

IV. FEM Formulation

The electromagnetic field distribution inside the conductive tissue region depends on the time varying magnetic flux density. The activation source is the electric field **E** induced in the tissues and expressed by using Faraday's law

$$\nabla \times \mathbf{E} = -\frac{\partial \mathbf{B}}{\partial t} \tag{1}$$

where **B** is the magnetic flux density, **H** is the magnetic field intensity, $\mathbf{B} = \mu \mathbf{H}$, μ is magnetic permeability.

According to

$$\nabla \mathbf{B} = 0 \tag{2}$$

and

$$\mathbf{B} = \nabla \times \mathbf{A} \tag{3}$$

where **A** is magnetic vector potential, from (1) is obtained

$$\nabla \times (\mathbf{E} - \frac{\partial \mathbf{A}}{\partial t}) = 0 \tag{4}$$

Using electric scalar potential V_ε, (4) can also be expressed as

$$\mathbf{E} = -\frac{\partial \mathbf{A}}{\partial t} - \nabla V_\varepsilon \tag{5}$$

The induced current density $\mathbf{J}_e$ satisfies the Ohm's law is

$$\mathbf{J}_e = \sigma \mathbf{E} = -\sigma(\frac{\partial \mathbf{A}}{\partial t} + \nabla V_\varepsilon) \tag{6}$$

According to Ampere law can be written

$$\nabla \times \mathbf{H} = \mathbf{J} - \sigma \mathbf{E} \tag{7}$$

or finally,

$$\nabla \times \frac{1}{\mu} \nabla \times \mathbf{A} = \mathbf{J} - \sigma(\frac{\partial \mathbf{A}}{\partial t} + \nabla V_\varepsilon) \tag{8}$$

Equation (8) is the governing equation for magnetic vector potential-electric scalar potential (A-V, A) formulation.

A three-dimensional harmonic and transient electromagnetic problem according FEM formulation was used for the field analysis.

Scheme used for the model formulation is shown in Fig.9. Ω is the whole domain. Ω_1 is the current source domain and Ω_3 is the stimulated tissue domain, in both domains the **A** and V_ε exists. Ω_2 is the surrounding free space with only magnetic vector potential distribution.

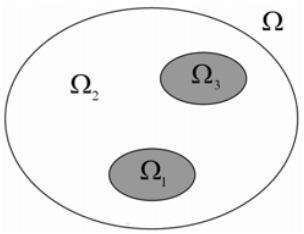

Fig. 9 Scheme used for the model formulation

Electromagnetic field source is coil region Ω_1 domain represented with its current densities.

Zero value Dirichlet boundary condition for the free space Ω_2 boundary is applied.

The finite element implementation of the A-V, A formulation has been carried out by using four-nodded, first-order, tetrahedral elements. The problem is solved by ANSYS software [5].

The electromagnetic properties of various tissues for frequency 10kHz is shown in Table1.

TABLE I
Electromagnetic Properties

Tissue	μ	σ (S/m)	ε (μF/m)
Brain White Matter	1	0.142	1
Brain Gray Matter	1	0.33	1
Cerebrospinal Fluid	1	1.53	1
Bone	1	0.0054	1
Muscle	1	0.11	1
Fat	1	0.04	1
Soft Tissue	1	0.173	1
Skin	1	0.435	1

The induced currents in tissue is expressed by (5).

Heating effect on the tissue can be calculated with Joule

heating Q.

$$Q = \rho J^2 \quad (9)$$

where $\rho=1/\sigma$, is specific electrical resistance.

V. Electromagnetic Field Modeling

Constructed realistic 3D anatomy models are imported in ANSYS software and the electromagnetic models are built according to the described FEM formulation. The electromagnetic model represents the organs field distribution under magnetic stimulation.

A. Thorax

The 3D model of human thorax under magnetic stimulation field with some inner organs in it is shown in Fig. 10.

Field source is a cylindrical coil. Coil dimensions are: external radius – 100mm, inner radius – 60mm and height – 20mm. Total current is 2000A.

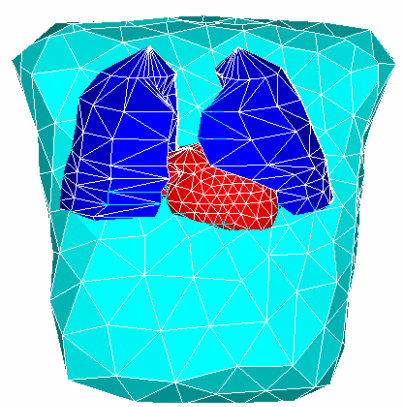

Fig. 10. 3D model of human thorax with inner organs.

Magnetic vector potential distribution and magnetic flux density distributions are shown in Fig.11. and Fig.12, respectively. Coil impact over the chest region can be seen by maximum values above the coil. Scalar electric potential distribution is shown in Fig 13.

Magnetic flux density on surface of inner organs is shown in Fig. 14. Flux density in heart volume only is shown in Fig. 15.

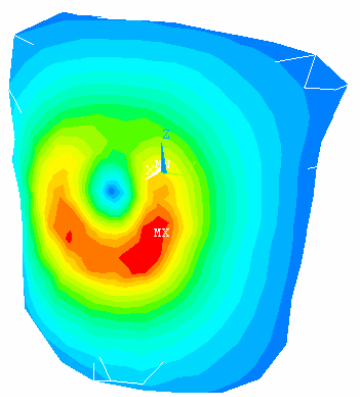

Fig. 11 Magnetic vector potential distribution

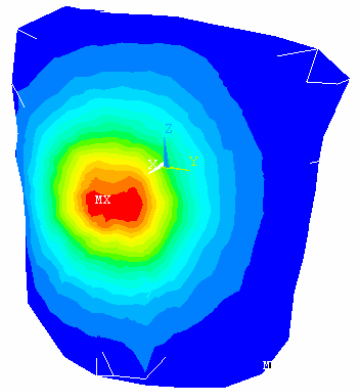

Fig. 12 Magnetic flux density distribution

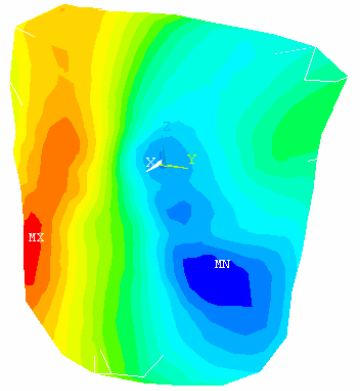

Fig. 13 Scalar electric potential distribution

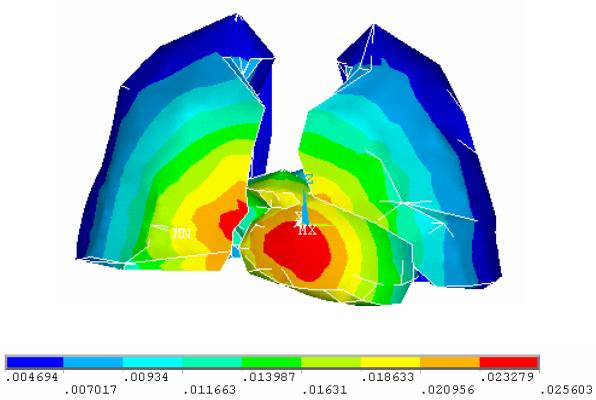

Fig. 14 Magnetic flux density distribution in inner organ volumes

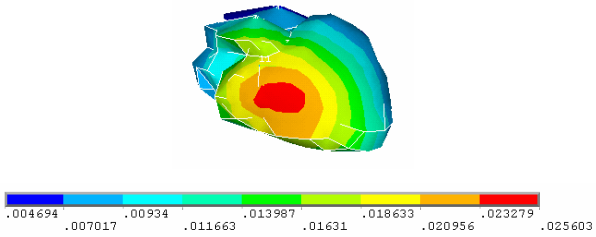

Fig. 15. Magnetic flux density (T) distribution in the heart volume

B. Head

The 3D model of human head with magnetic stimulation coil is shown in Fig. 17. The model consists of scalp, skull, cerebrospinal fluid and brain, shown in Fig. 16. The relative permeability and resistivity of the tissues are shown in Table 1.

Field source is a cylindrical coil. Coil dimensions are: external radius – 60mm, inner radius – 50mm and height – 8mm. Total current is 400A.

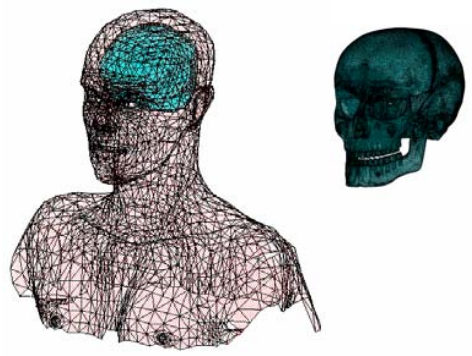

Fig. 16. 3D model of human head with brain and skull volumes

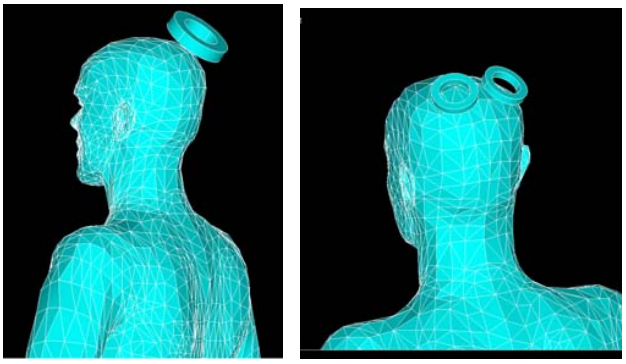

Fig. 17. TMS coil position over the head

Analyzed magnetic vector potential distribution is shown in Fig. 18. Magnetic flux density over the brain volume enclosure surface is demonstrated in Fig.19.

Joule heating calculated for each element of brain region using (5) is shown in Fig. 20.

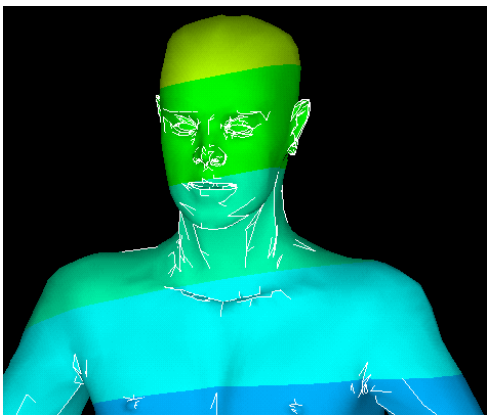

Fig. 18. Magnetic vector potential distribution in model skin surface

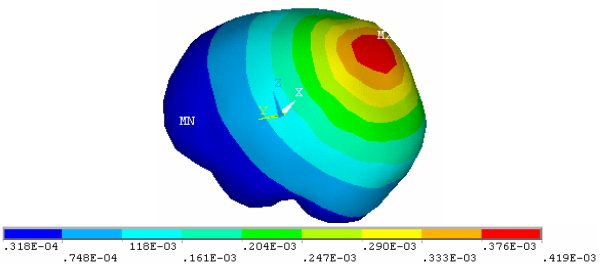

Fig. 19. Magnetic flux density over the brain volume enclosure surface

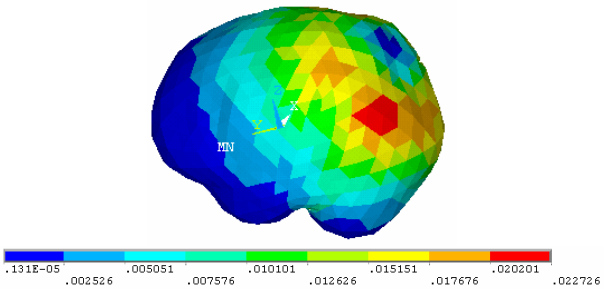

Fig. 20. Joule heating in each element of treated organ

Second field source is a "8-sahaped" or butterfly coils. Both coils have same dimensions as follows: external radius – 40mm, inner radius – 35mm and height – 6mm. Angle between coils axes is 15 deg., total current for each is 180A.

Magnetic flux density over the brain volume enclosure surface with butterfly coils is demonstrated in Fig.21.

Joule heating for that case is shown in Fig. 22.

Butterfly coil results in a more focal pattern of field distribution as shown in Fig.19 and Fig.21.

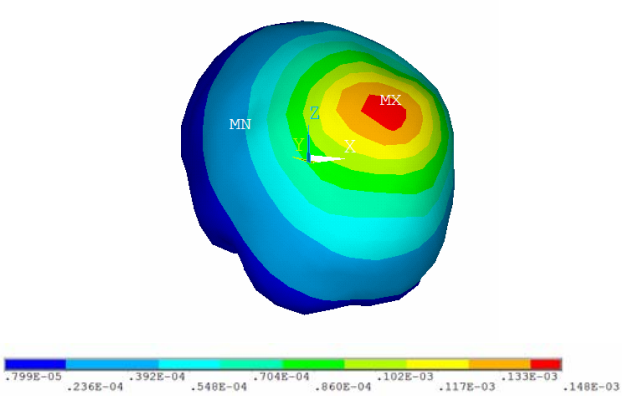

Fig. 21. Magnetic flux density over the brain volume enclosure surface with butterfly coil

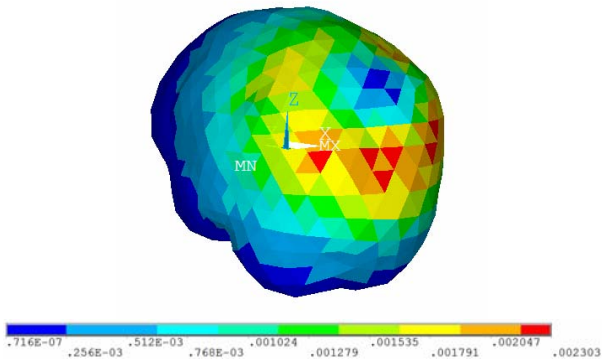

Fig. 22. Joule heating in each brain element with butterfly coil

VI. Conclusion

In this paper we develop a method for automatic 3D geometry model building of anatomical objects. The method uses image data acquired by medical diagnostic equipment and bioimpedance measurements.

Electromagnetic field distribution in 3D human anatomy tissue objects is presented. Electromagnetic field distribution is investigated by FEM using magnetic vector potential and scalar electric potential (A-V, A) formulation, realized with computer software ANSYS.

Quantitative results for electromagnetic and thermal field distribution in inner organs can be easily made. Complete procedure of electromagnetic field model building is applicable for device and process optimization due to a desired electromagnetic or corresponding thermal impact over a known object.

Acknowledgment

This research is supported by the National Science Fund of the Ministry of Education and Science of Bulgaria under Contract "D002-157/2008".

References

[1] S. Zachow, M. Zilske, H-C. Hege. 3D Reconstruction of Individual Anatomy from Medical Image Data: Segmentation and Geometry *Proceedings of the 25th CADFEM Users' Meeting 2007*, Congress Center Dresden, Germany, November 21-23, 2007.

[2] K. Neubert et al. Model-Based Autosegmentation of Brain Structures in the Honeybee Using Statistical Shape Models, *Proc. 8th Int. Congr. of Neuroethology,* 2007

[3] J. Cebral , R. Lohner. "From Medical Images to Anatomically Accurate Finite Element Grids". *Int. Journal For Numerical Methods in Engineering*, 51(8), 2001, pp. 985–1008.

[4] J. Zheng , L. Li, X. Huo. „Analysis of Electric Field in Real Head Model during Transcranial Magnetic Stimulation". *Proceedings of the 2005 IEEE Engineering in Medicine and Biology,* 27th Annu. Conf., Shang Hai, 2005.

[5] ANSYS Release 12.0 Documentation.

[6] P. Basser, B. Roth. "New currents in electrical stimulation of excitable tissues". *Annu. Rev. Biomed. Eng*., 02, 2000, pp. 377-397.

[7] P. Tofts, "The distribution of induced current in magnetic stimulation of the nervous system." *Phys. Med. Biol*. 35, 1990, pp. 1119-1128.

[8] J. Ruohonen, P. Ravazzani, J. Nilsson, M. Panizza, F. Grandori and G. Tognola. "A volume-conduction analysis of magnetic stimulation of peripheral nerves." *IEEE Trans. Biomed. Eng*. 1996, 43, pp. 669-678.

[9] P. Karu, M. Stuchly. "Quasi-static electric field in a cylindrical volume conductor induced by external coils." *IEEE Trans. Biomed. Eng*., 41, 1994, pp. 151-158.

[10] B. Roth, J. Saypol, M. Hallet, L. Cohen. "A theoretical calculation of the electric field induced by magnetic stimulation of a peripheral nerve", *Muscle & Nerve*, 13, 1994, pp. 734-741.

[11] S. Nagarajan, M. Durand. "Analysis of magnetic stimulation of a concentric axon in a nerve bundle." *IEEE Trans. Biomed. Eng.,* 42, 1995, pp. 926-932.

[12] B. Roth, J. Saypol, M. Hallet, L. Cohen. "A theoretical calculation of the electric field induced in the cortex during magnetic stimulation", *Electroenceph. Clin. Neurophysiol*, 81, 1991, pp. 47-56.

[13] P. Ragan, W. Wang, S. Eisenbrg. „Magnetically induced currents in the canine Heart. A finite element study", *IEEE Trans Biomed Eng*, 1995, 42, pp. 1110-1116.

[14] V. Krasteva, S. Papazov, I. Daskalov. "Magnetic Stimulation for non-homogeneous biological structures", *BioMed Eng Online* 2002, pp. 1:3.

[15] P. Miranda, M. Hallet, P. Basser. The electric field induced in the brain by magnetic stimulation: "A 3D Finite-element analysis of the effect of tissue heterogeneity and anisotropy", *IEEE Trans Biomed Eng*, 50, 2003, pp. 1074-1085.

[16] J. Malmivuo, J. Plonsey. *Bioelectromagnetism*. Oxford University Press, New York-Oxford 1995.

[17] U. Pliquett, S. Gallo, S. Hui, Ch. Gusbeth, E. Neumann. "Local and transient structural changes in stratum corneum at high electric fields: contribution of Joule heating", *Bioelectrochem*., Vol. 67, 2005. pp. 37-46.